Published in final edited form as:
Invest Ophthalmol Vis Sci. 2009 February ; 50(2): 765–770. doi:10.1167/iovs.08-2501.

Enhanced Inflow and Outflow Rates Despite Lower IOP in Bestrophin-2-Deficient Mice

Youwen Zhang[1], **Bryan R. Davidson**[2], **W. Daniel Stamer**[1,3], **Jennifer K. Barton**[2,4], **Lihua Y. Marmorstein**[1,4], and **Alan D. Marmorstein**[1,5]

[1] Department of Ophthalmology and Vision Science, University of Arizona, Tucson, Arizona

[2] Department of Electrical and Computer Engineering, University of Arizona, Tucson, Arizona

[3] Department of Pharmacology, University of Arizona, Tucson, Arizona

[4] Department of Physiology, University of Arizona, Tucson, Arizona

[5] College of Optical Sciences, University of Arizona, Tucson, Arizona

Abstract

Purpose—Bestrophin-2 (Best2), a putative Cl^- channel is expressed in the nonpigmented epithelium (NPE). Disruption of Best2 in mice results in a diminished intraocular pressure (IOP). Aqueous humor dynamics were compared in *Best2*$^{+/+}$ and *Best2*$^{-/-}$ mice, to better understand the contribution of Best2 to IOP.

Methods—Measurements of IOP, episcleral venous pressure (EVP), conventional outflow facility (C_t), aqueous humor production (F_a), and anterior chamber volume (V_a) were made using anterior chamber cannulation. Conventional (F_c) and uveoscleral outflow (F_u), and rate of aqueous humor turnover, were calculated from measured data. The anterior chamber was examined in live mice by optical coherence tomography (OCT) and postmortem by light microscopy.

Results—IOP in *Best2*$^{-/-}$ mice was lower compared with *Best2*$^{+/+}$ littermates. EVP was unchanged. Since Best2 is expressed in NPE cells, the hypothesis was that Best2 is involved in generating aqueous flow. However, F_a in *Best2*$^{-/-}$ mice was increased by ~73% compared with *Best2*$^{+/+}$ mice. This was accompanied by increases in F_c and F_u. Aqueous humor turnover was enhanced more than twofold in *Best2*$^{-/-}$ mice. No evidence of developmental structural changes was noted.

Conclusions—Best2 appears to antagonize the formation of aqueous humor and cause an inhibition of both F_c and F_u, despite being expressed only in NPE cells. These data support the hypothesis that the inflow and outflow pathways communicate via soluble agents present in the aqueous humor and implicate Best2 as a critical mediator of that communication.

The production of aqueous humor by the ciliary epithelium requires the transepithelial movement of H_2O and various ions. H_2O transport by the nonpigmented epithelium (NPE) like that of the retinal pigment epithelium (RPE) and transporting epithelia in the colon, is thought to be coupled to Cl^- transport.[1,2] While there is evidence of the participation of as many as three distinct Cl^- channels in aqueous humor formation, CLC-3 is the only candidate to date for which there is direct evidence of involvement.[3,4]

Corresponding author: Alan D. Marmorstein, University of Arizona, Department of Ophthalmology and Vision Science, 655 N. Alvernon Way, Suite 108, Tucson, AZ 85711; amarmorstein@eyes.arizona.edu.

Disclosure: **Y. Zhang**, None; **B.R. Davidson**, None; **W.D. Stamer**, None; **J.K. Barton**, None; **L.Y. Marmorstein**, None; **A.D. Marmorstein**, None

Bestrophins are a recently recognized family of proteins that have gained significant interest as potential Ca^{2+}-activated Cl^- channels (CaCCs), although this function is somewhat controversial.[5,6] Recently, our laboratory demonstrated that mice in which the gene *Best2*, encoding bestrophin-2 (Best2) was disrupted exhibit a significantly lower IOP than *Best2*$^{+/+}$ littermates.[7] Best2 is uniquely expressed in the basolateral plasma membrane of the NPE in the eye, as well as in several other tissues, including the transporting epithelium of the colon.[7] In addition to their putative CaCC activity, bestrophins have been proposed to function as voltage-dependent anion or bicarbonate channels,[6,8] regulators of voltage-dependent Ca^{2+} channels,[5,9,10] and regulators of Na^+ dependent H^+ transport (Zhang et al., unpublished observations, 2008). The diminished IOP observed in *Best2*$^{-/-}$ mice suggests that Best2 may serve as one of the Cl^- channels responsible for driving aqueous humor formation.

To test the hypothesis that Best2 is a Cl^- channel necessary for aqueous formation, we performed a comprehensive study of aqueous dynamics in *Best2*$^{-/-}$ mice, anticipating that aqueous formation would be diminished. To our surprise, we found that although IOP in these mice is lower in comparison to *Best*$^{+/+}$ mice, the rate of aqueous formation, F_a, is significantly increased as is drainage through both the conventional (F_c) and uveoscleral (F_u) outflow pathways. Morphologic inspection of the anterior chamber did not identify any developmental or anatomic changes that would explain this phenomenon. Based on these data, we propose that Best2 does not participate in, but antagonizes the formation of aqueous humor, and that there is a communicative link between the ciliary epithelia and the outflow pathways that involves signaling via the only common component of the two, the aqueous humor. Finally, we conclude that these data continue a string of recent findings that are inconsistent with Bestrophins functioning in vivo as CaCCs,[5,11,12] and are more consistent with the hypothesis that bestrophins are regulators of ion transport.

Methods

IOP Measurements

Mice deficient in *Best2* have been reported previously.[7] All experiments were performed in accordance with the ARVO Statement for the Use of Animals in Ophthalmic and Vision Research on mice aged 2 to 4 months. IOP was measured in mice by cannulation of the anterior chamber, as described previously,[7,13–15] by using Avertin anesthesia (300 mg/kg injected intraperitoneally). In brief, the anterior chamber was cannulated with a borosilicate glass microneedle, filled with Hanks' balance salt solution (HBSS) and connected to a pressure transducer (BLPR; World Precision Instruments, Sarasota, FL). The signal was amplified (Bridge8 amplifier; World Precision Instruments), converted from analog to digital (Iworx model 108 converter; CB Sciences, Dover, NH), and recorded (LabScribe software ver. 1.6; CB Sciences). IOP was recorded for a period of >90 seconds, and the IOP was determined from the average of each recording. Recordings were discarded if the variance during the recording period exceeded 1 mm Hg or did not immediately return to zero after withdrawal of the needle. All measurements were performed between 2 and 6 PM, to avoid diurnal pressure variation. The apparatus was calibrated by using a fluid reservoir the height of which could be adjusted to generate a series of known pressures.

Determination of Aqueous Humor Production

The rate of aqueous humor formation was determined by dilution of a fluorescent perfusate according to the method of Aihara et al.[13] substituting 5 μg/mL FITC-Dextran (70 kDa) for rhodamine dextran. Perfusion pressure was maintained at EVP so that pressure-dependent outflow was reduced to zero. Fluorescence was determined on a multilabel counter (Wallac, Victor3 1420; PerkinElmer Life Sciences, Wellesley, MA), with excitation and emission wavelengths of 485 and 535 nm, respectively. Aqueous production (F_a) was calculated based

on the aspiration rate (3 μL/min) and the ratio of the concentration of FITC-dextran in the perfusion outflow fluid (C_o) to the concentration of FITC-dextran in the perfusion inflow fluid (C_i), according to Aihara et al[13]:

$$F_a = 3\mu L \cdot \min^{-1}(1 - C_o/C_i). \quad (1)$$

Measurement of Conventional Outflow Facility

Conventional outflow facility (C_t) was determined according to Aihara et al.,[13] with the same infusion system used to measure IOP and aqueous production. All fluid within the infusion system was replaced with physiological saline. The measurement was based on measuring total outflow volume (V_t) for a period of 10 minutes at two different levels of IOP (25 and 35 mm Hg), maintained by altering the reservoir height. C_t was determined according to the following equation:

$$C_t = 0.01 \times (V_{t=35} - V_{t=25})\mu L \cdot \min^{-1}/\text{mm Hg}. \quad (2)$$

Determination of Conventional and Uveoscleral Outflow

IOP, EVP, and C_t were measured and averaged for each genotype. Using these data, the conventional outflow (F_c) was calculated as:

$$F_c = C_t \times (\text{IOP} - \text{EVP}). \quad (3)$$

Uveoscleral outflow (F_u) was then calculated according to the modified Goldmann equation:

$$F_u = F_a - C_t \times (\text{IOP} - \text{EVP}). \quad (4)$$

Anterior Chamber Volume and Aqueous Humor Turnover Rate

Anterior chamber volume (V_a) was determined by aspiration of the aqueous humor at a rate of 100 nL/s, according to Aihara et al.[13] Aspiration was deemed complete when the central border of the iris was observed by dissecting microscope to make contact with the cornea. The turnover rate (% $\cdot$ min^{-1}) was calculated as:

$$\text{Turnover rate} = 100 \times F_a/V_a. \quad (5)$$

Statistical Analysis

Data from *Best2*$^{+/+}$ and *Best2*$^{-/-}$ mice were compared by using the two-tailed, homoscedastic *t*-test function (Excel 2004 for MAC; Microsoft, Redmond, WA).

Histology

Two-month-old mice were fixed by intracardiac perfusion with half-strength Karnovsky's fixative (2.5% glutaraldehyde and 2% paraformal-dehyde in 0.1 M cacodylate buffer [pH 7.2]). The eyes were enucleated and further fixed by immersion in half strength Karnovsky's fixative for an additional 18 hours, after which they were transferred to 0.1 M cacodylate buffer (pH 7.2). The eyes were then postfixed with 1% osmium tetroxide, dehydrated in a graded series of alcohols, and embedded in Spurr's resin. Semi-thin sections (0.5 μm) were cut on a microtome (Reichert Ultracut; Leica, Deerfield, IL) and stained with toluidine blue. Sections

were inspected with a microscope (E-600; Nikon, Tokyo, Japan) and photographed with a color CCD camera.

Optical Coherence Tomography

Two- to 4-month-old mice were anesthetized with Avertin (250 mg/kg IP) and placed on a mechanical stage that permitted movement along two axes. The anterior chamber was imaged (OCP930SR Spectral Radar OCT Imaging System; Thorlabs, Newton, NJ) with a 930-nm center wavelength light source and an axial resolution 4.5 μm in tissue. Cross-sectional images were recorded in the nasal–temporal plane as well as the superior–inferior plane. Pixel images (500 × 512; *x*–*z*) were captured at maximum pupillary diameter and corrected for asymmetries in *x*–*z* spacing (Photoshop 7.01; Adobe Systems, San Jose, CA). Measurements of anterior chamber depth and corneal thickness were made from distortion-corrected images obtained along both the nasal–temporal and superior–inferior axis using Image J software (developed by Wayne Rasband, National Institutes of Health, Bethesda, MD; available at http://rsb.info.nih.gov/ij/index.html).

Results

Effect of Best2 Disruption on IOP

In our previous study,[7] we observed that IOP was diminished in *Best2*$^{-/-}$ mice in comparison to their *Best2*$^{+/+}$ littermates. Since that initial report, we have increased the number of animals on which we have performed measurements of IOP. In the current study, The measured IOP in *Best2*$^{+/+}$ was 11.70 ± 0.16 mm Hg (mean ± SE, n = 31) and for *Best2*$^{-/-}$ it was 10.22 ± 0.16 mm Hg (mean ± SE, n = 55), a significant ($P < 0.0001$) difference of 1.48 mm Hg (Fig. 1, Table 1).

Measurement of Aqueous Humor Formation

According to the modified Goldmann equation, IOP = $[(F_a - F_u)/C_t]$ + EVP. In our prior study[7] we measured EVP in *Best2*$^{+/+}$ and *Best2*$^{-/-}$ mice and found no difference with both groups having an EVP of 6.3 ± 0.3 mm Hg (Table 1). Since EVP between *Best2*$^{+/+}$ and *Best2*$^{-/-}$ mice are identical, the difference in IOP must arise from differences in F_a or C_t. Combined with our observation that Best2 is expressed only in NPE cells in the eye, we hypothesized that the diminished IOP is the result of a diminished rate of aqueous humor formation.

To test our hypothesis, we used a modification of the method of Aihara et al.,[13] in which the anterior chamber of the eye is cannulated, clamped at EVP, and perfused with a physiologic salt solution containing a 70-kDa FITC-dextran. By observing dilution of the fluorescence emission of the perfusion outflow fluid versus that of the inflow fluid, we determined F_a. In *Best2*$^{+/+}$ mice F_a was 0.160 ± 0.047 μL/min (mean ± SD, n = 9; Fig. 2A, Table 1), similar to the 0.18 ± 0.05 μL/min reported by Aihara et al. in NIH Swiss white mice. Unexpectedly, F_a in Best2$^{-/-}$ mice was 0.277 ± 0.069 μL/min (mean ± SD, n = 9; Fig. 2A, Table 1), a significant ($P < 0.001$) increase (73%) over the *Best2*$^{+/+}$ mice.

Measurement of Conventional Outflow Facility

Based on the modified Goldmann equation (equation 4), for IOP to be diminished without altering EVP, either F_a must be diminished or F_u and C_t must be increased. Since F_a was significantly increased for *Best2*$^{-/-}$ mice, and F_u cannot be measured directly, we next measured C_t (Fig. 2B, Table 1). Again employing the methods of Aihara et al.[13] we observed in *Best2*$^{+/+}$ mice, C_t was 0.0050 ± 0.0015 μL · min^{-1}/mm Hg (mean ± SD, n = 23, Fig. 2B, Table 1), nearly identical with the 0.0051 μL · min^{-1}/mm Hg reported by Aihara et al. in NIH

Swiss white mice. Of interest, in *Best2*$^{-/-}$ mice, C_t was 0.0085 ± 0.0026 μL · min^{-1}/mm Hg (mean ± SD, n = 23, Fig. 2B, Table 1), a significant ($P < 0.001$) increase (70%) compared with *Best2*$^{+/+}$ mice.

Having obtained measured values for IOP, EVP, F_a, and C_t, we calculated F_c and F_u by using equations 3 and 4, respectively. As shown in Table 1, F_c was 0.027 and 0.033 μL · min^{-1} in *Best2*$^{+/+}$ and *Best2*$^{-/-}$ mice, respectively, a 22% increase in F_c for *Best2*$^{-/-}$ mice. F_u was calculated to be 0.133 and 0.211 L · min^{-1} in *Best2*$^{+/+}$ and *Best2*$^{-/-}$ mice respectively, a 59% increase in *Best2*$^{-/-}$ mice. These results indicate that both pressure-dependent and independent outflow appears to overcompensate for the increase in F_a in *Best2*$^{-/-}$ mice resulting in an IOP that is lower in *Best2*$^{-/-}$ mice than in *Best2*$^{+/+}$ mice, despite the 73% increase in F_a in *Best2*$^{-/-}$ mice.

Anatomy of the Angle

The increase in C_t was perplexing, considering that Best2 is expressed only in the NPE and not by cells in drainage tissues. One potential explanation is anatomic differences or abnormalities resulting from a lack of Best2. A postmortem examination of the angles of *Best2*$^{+/+}$ and *Best2*$^{-/-}$ mice identified no gross anatomic abnormalities in outflow structures; however, we occasionally observed an expanded TM and deposits of pigment in the TM of *Best2*$^{-/-}$ mice (Fig. 3).

In parallel studies, we examined the anterior chamber of live mice using OCT (Fig. 4). No difference was observed in the thickness of the cornea (Table 2). However, the anterior chamber depth (ACD) measured from the inner surface of the cornea to the anterior surface of the lens capsule was 496 μm in *Best2*$^{+/+}$ mice (n = 12) but only 458 μm in *Best2*$^{-/-}$ mice (n = 15), a decrease of nearly 40 μm (Fig. 4, Table 2).

To determine anterior chamber volume (V_a), we used the aqueous humor aspiration method of Aihara et al.[13] Consistent with the change observed in ACD, the anterior chamber volume was decreased by 17% in *Best2*$^{-/-}$ mice (Table 1). Based on V_a and F_a, we calculated the turnover rate of aqueous humor by using equation 5. Turnover in *Best2*$^{+/+}$ and *Best2*$^{-/-}$ mice was 3.5% · min^{-1} and 7.4% · min^{-1} respectively; a 2.1-fold increase in the *Best2*$^{-/-}$ mice.

Discussion

In our study, *Best2*$^{-/-}$ mice exhibited diminished IOP, despite a ~73% increase in F_a and a more than twofold increase in the rate of aqueous turnover. The increase in F_a was overcompensated for by enhanced drainage. Both F_c and F_u were increased, although a more significant portion of the aqueous flow drained via F_u than F_c in the *Best2*$^{-/-}$ mice. Based on the antagonistic effect of Best2 on F_a we conclude that Best2 is not one of the Cl^- channels involved in aqueous humor formation, leaving us with the question of how Best2 antagonizes aqueous humor production.

The hypothesis that bestrophins function as CaCCs[16] arose from the observation that individuals with Best vitelliform macular dystrophy (BVMD), due to mutations in *BEST1*, exhibit a diminished electrooculogram light peak.[17] This response is generated by a Cl^- conductance across the basolateral surface of the retinal pigment epithelium[18] (RPE) where Best1 is normally expressed.[19] Support for this idea came from heterologous expression studies showing bestrophin-specific CaCC activity that was diminished or absent in all mutant forms of Best1 tested.[16] However, disruption of Best1 does not diminish the light peak in mice,[11] and the diminished CaCC activity exhibited by mutant Best1 does not explain how different Best1 mutants cause four clinically distinct diseases.

A second hypothesis for bestrophin function is that this family of proteins functions as regulators of ion transport.[5,6,9–11] We have shown that L-type voltage dependent Ca^{2+} channels (VDCCs) are required for the light peak,[9,11,20] and that Best1 and Best1 mutants exert specific effects on the kinetics of VDCCs,[9,11] a finding recently confirmed by Yu et al.,[10] who also demonstrated a physical interaction of Best1 with the β3 subunit of VDCC channels. Thus, Best2 may play a role in regulating Ca^{2+} signaling, similar to what we have proposed for Best1.[5,9,11] The NPE is in close physical contact with the pigment epithelium (PE), working in tandem to generate the aqueous flow. According to Mitchell et al.[21] PE cells release ATP due to cell swelling, which results in activation of a hypothesized Ca^{2+} dependent negative feedback loop sending Cl^- into the stroma.[2,21] ATP stimulates P2Y2 receptors in PE cells to trigger Ca^{2+} release. In mice, disruption of Best1 results in an increase in $[Ca^{2+}]_i$ compared with wild-type mice in response to extracellular ATP, suggesting that Best1 functions to regulate intracellular Ca^{2+} signaling. Although Best2 is in the NPE and not the PE, these cells communicate through an extensive network of GAP junctions.[22] Perhaps, Best2 normally acts as the governor of the negative feedback loop altering Ca^{2+} signaling to promote aqueous resorption to control the desired rate of aqueous flow. In its absence this failure to properly regulate Ca^{2+} signaling could result in a diminished rate of Cl^- recycling and thus enhanced aqueous production.

The increase in F_a observed in *Best2*$^{-/-}$ mice in the present study should logically have led to an increase in IOP. However, there was an overcompensating effect on the conventional outflow facility that resulted in a diminished IOP. How could this occur? We observed no obvious anatomic changes such as breaks in the inner wall of Schlemm's canal or larger spaces between ciliary muscle bundles that would account for elevated drainage through either the conventional or uveoscleral pathways. However, we did observe TM tissues that appeared expanded, perhaps the result of enhanced outflow. Such a difference may be more obvious if eyes are fixed under pressure. If there is no dramatic developmental or structural abnormality in the angle, then the increase in C_t must have been functional and have been triggered by the increase in F_a. Others have proposed that the ciliary body communicates with the TM via the aqueous humor.[23–25] The mechanism underlying this putative communication is unknown although bioactive peptides have been suggested as one possible mechanism.[23–25] Changes in $[Ca^{2+}]_i$ could have profound effects not only on ion transport properties of NPE cells, but may alter secretion of bioactive peptides,[26,27] or perhaps alter the ionic composition,[21,28–30] and/or the viscosity[31] of the aqueous humor in a manner promoting enhanced outflow. Further studies are needed to test these hypotheses and to better understand the role of Best2 and how it can affect outflow.

It has been noted that there is an enormous variation in the ratio of drainage through the conventional and uveoscleral pathways in different species. In rabbits, F_a, is <10% of F_u whereas mice are at the other end of the spectrum with ~80% of drainage flowing through the uveoscleral pathway.[13,31] Humans and other primates range from 4% to 60%,[32] depending on age. In general, younger primates make greater use of the uveoscleral pathway than older ones. In the present study we have confirmed that mice are prolific in their use of uveoscleral drainage, with F_u constituting 83% of total outflow in our wild-type mice and 88% in the *Best2*$^{-/-}$ mice. Although Lindsey and Weinreb[33] have qualitatively demonstrated that the mouse has a uveoscleral pathway, the small size of the mouse eye has stymied efforts to directly measure F_u. As a result, F_u in the mouse is calculated indirectly based on the assumption that drainage must be split between the conventional and uveoscleral pathways (see equation 4). The absence of Best2 causes a further increase in F_u such that it constitutes 88% of total drainage. However, this does not alter our hypothesis regarding how outflow is enhanced. Bioactive peptides, ion composition, and aqueous humor viscosity could all play roles in enhancing uveoscleral drainage.

In summary, we have shown that disruption of Best2 in mice results in a significant decrease in IOP despite a 73% increase in F_a. Therefore, Best2 is a potent antagonist of aqueous humor production. The enhanced production of aqueous humor is overcompensated for by an increase in both conventional and uveoscleral drainage. Since Best2 is expressed uniquely in the NPE and there is no obvious anatomic reason for increased outflow, these data imply a communicative link between the ciliary body and the out-flow pathway that is modulated by Best2. Therefore, drugs that target Best2 function would appear to be novel candidates for the treatment of glaucoma.

Acknowledgments

The authors thank Nicholas Delamere for helpful discussions.

Supported by National Institutes of Health Grants EY13160 (ADM) and EY13847 (LYM), the Macular Vision Research Foundation (ADM), a Career Development Award (LYM), and an unrestricted grant to the Department of Ophthalmology and Vision Science at the University of Arizona from Research to Prevent Blindness.

References

1. Civan MM, Macknight AD. The ins and outs of aqueous humour secretion. Exp Eye Res 2004;78:625–631. [PubMed: 15106942]
2. Do CW, Civan MM. Basis of chloride transport in ciliary epithelium. J Membr Biol 2004;200:1–13. [PubMed: 15386155]
3. Do, CW.; Civan, MM. Acta Physiol. Vol. 187. Oxf: 2006. Swelling-activated chloride channels in aqueous humour formation: on the one side and the other; p. 345-352.
4. Coca-Prados M, Sanchez-Torres J, Peterson-Yantorno K, Civan MM. Association of ClC-3 channel with Cl− transport by human non-pigmented ciliary epithelial cells. J Membr Biol 1996;150:197–208. [PubMed: 8661780]
5. Marmorstein AD, Kinnick TR. Focus on molecules: bestrophin (Best-1). Exp Eye Res 2007;85:423–424. [PubMed: 16720022]
6. Hartzell HC, Qu Z, Yu K, Xiao Q, Chien LT. Molecular physiology of bestrophins: multifunctional membrane proteins linked to best disease and other retinopathies. Physiol Rev 2008;88:639–672. [PubMed: 18391176]
7. Bakall B, McLaughlin P, Stanton JB, Hartzell HC, Marmorstein LY, Marmorstein AD. Bestrophin-2 is involved in the generation of intraocular pressure. Invest Ophthalmol Vis Sci 2008;49(4):1563–1570. [PubMed: 18385076]
8. Qu Z, Hartzell HC. Bestrophin Cl− channels are highly permeable to HCO3. Am J Physiol Cell Physiol 2008;294:C1371–C1377. [PubMed: 18400985]
9. Rosenthal R, Bakall B, Kinnick T, et al. Expression of bestrophin-1, the product of the VMD2 gene, modulates voltage-dependent Ca2+ channels in retinal pigment epithelial cells. FASEB J 2006;20:178–180. [PubMed: 16282372]
10. Yu K, Xiao Q, Cui G, Lee A, Hartzell HC. The best disease-linked Cl− channel hBest1 regulates Ca V 1 (L-type) Ca2+ channels via src-homology-binding domains. J Neurosci 2008;28:5660–5670. [PubMed: 18509027]
11. Marmorstein LY, Wu J, McLaughlin P, et al. The light peak of the electroretinogram is dependent on voltage-gated calcium channels and antagonized by bestrophin (best-1). J Gen Physiol 2006;127:577–589. [PubMed: 16636205]
12. Burgess R, Millar ID, Leroy BP, et al. Biallelic mutation of BEST1 causes a distinct retinopathy in humans. Am J Hum Genet 2008;82:19–31. [PubMed: 18179881]
13. Aihara M, Lindsey JD, Weinreb RN. Aqueous humor dynamics in mice. Invest Ophthalmol Vis Sci 2003;44:5168–5173. [PubMed: 14638713]
14. John SW, Hagaman JR, MacTaggart TE, Peng L, Smithes O. Intraocular pressure in inbred mouse strains. Invest Ophthalmol Vis Sci 1997;38:249–253. [PubMed: 9008647]

15. Husain S, Whitlock NA, Rice DS, Crosson CE. Effects of latanoprost on rodent intraocular pressure. Exp Eye Res 2006;83:1453–1458. [PubMed: 17027754]
16. Sun H, Tsunenari T, Yau KW, Nathans J. The vitelliform macular dystrophy protein defines a new family of chloride channels. Proc Natl Acad Sci USA 2002;99:4008–4013. [PubMed: 11904445]
17. Cross HE, Bard L. Electrooculography in Best's muscular dystrophy. Am J Ophthalmol 1974;77:46–50. [PubMed: 4824173]
18. Gallemore RP, Steinberg RH. Effects of DIDS on the chick retinal pigment epithelium. II. Mechanism of the light peak and other responses originating at the basal membrane. J Neurosci 1989;9:1977–1984. [PubMed: 2723762]
19. Marmorstein AD, Marmorstein LY, Rayborn M, Wang X, Hollyfield JG, Petrukhin K. Bestrophin, the product of the Best vitelliform macular dystrophy gene (VMD2), localizes to the basolateral plasma membrane of the retinal pigment epithelium. Proc Natl Acad Sci U S A 2000;97:12758–12763. [PubMed: 11050159]
20. Wu J, Marmorstein AD, Striessnig J, Peachey NS. Voltage-dependent calcium channel CaV1.3 subunits regulate the light peak of the electroretinogram. J Neurophysiol 2007;97:3731–3735. [PubMed: 17376851]
21. Mitchell CH, Carre DA, McGlinn AM, Stone RA, Civan MM. A release mechanism for stored ATP in ocular ciliary epithelial cells. Proc Natl Acad Sci U S A 1998;95:7174–7178. [PubMed: 9618558]
22. Calera MR, Topley HL, Liao Y, Duling BR, Paul DL, Goodenough DA. Connexin43 is required for production of the aqueous humor in the murine eye. J Cell Sci 2006;119:4510–4519. [PubMed: 17046998]
23. Potter DE, Russell KR, Manhiani M. Bremazocine increases C-type natriuretic peptide levels in aqueous humor and enhances outflow facility. J Pharmacol Exp Ther 2004;309:548–553. [PubMed: 14742737]
24. Coca-Prados M, Escribano J, Ortego J. Differential gene expression in the human ciliary epithelium. Prog Retin Eye Res 1999;18:403–429. [PubMed: 10192520]
25. Coca-Prados M, Escribano J. New perspectives in aqueous humor secretion and in glaucoma: the ciliary body as a multifunctional neuroendocrine gland. Prog Retin Eye Res 2007;26:239–262. [PubMed: 17321191]
26. Cullinane AB, Leung PS, Ortego J, Coca-Prados M, Harvey BJ. Renin-angiotensin system expression and secretory function in cultured human ciliary body non-pigmented epithelium. Br J Ophthalmol 2002;86:676–683. [PubMed: 12034692]
27. Krautheim A, Rustenbeck I, Steinfelder HJ. Phosphatase inhibitors induce defective hormone secretion in insulin-secreting cells and entry into apoptosis. Exp Clin Endocrinol Diabetes 1999;107:29–34. [PubMed: 10077352]
28. Speake T, Elliott AC. Modulation of calcium signals by intracellular pH in isolated rat pancreatic acinar cells. J Physiol 1998;506:415–430. [PubMed: 9490869]
29. Speake T, Yodozawa S, Elliott AC. Modulation of calcium signalling by intracellular pH in exocrine acinar cells. Eur J Morphol 1998;36(Suppl):165–169. [PubMed: 9825915]
30. Yao H, Haddad GG. Calcium and pH homeostasis in neurons during hypoxia and ischemia. Cell Calcium 2004;36:247–255. [PubMed: 15261480]
31. Crowston JG, Lindsey JD, Aihara M, Weinreb RN. Effect of latanoprost on intraocular pressure in mice lacking the prostaglandin FP receptor. Invest Ophthalmol Vis Sci 2004;45:3555–3559. [PubMed: 15452062]
32. Fautsch MP, Johnson DH. Aqueous humor outflow: what do we know? Where will it lead us? Invest Ophthalmol Vis Sci 2006;47:4181–4187. [PubMed: 17003404]
33. Lindsey JD, Weinreb RN. Identification of the mouse uveoscleral outflow pathway using fluorescent dextran. Invest Ophthalmol Vis Sci 2002;43:2201–2205. [PubMed: 12091417]

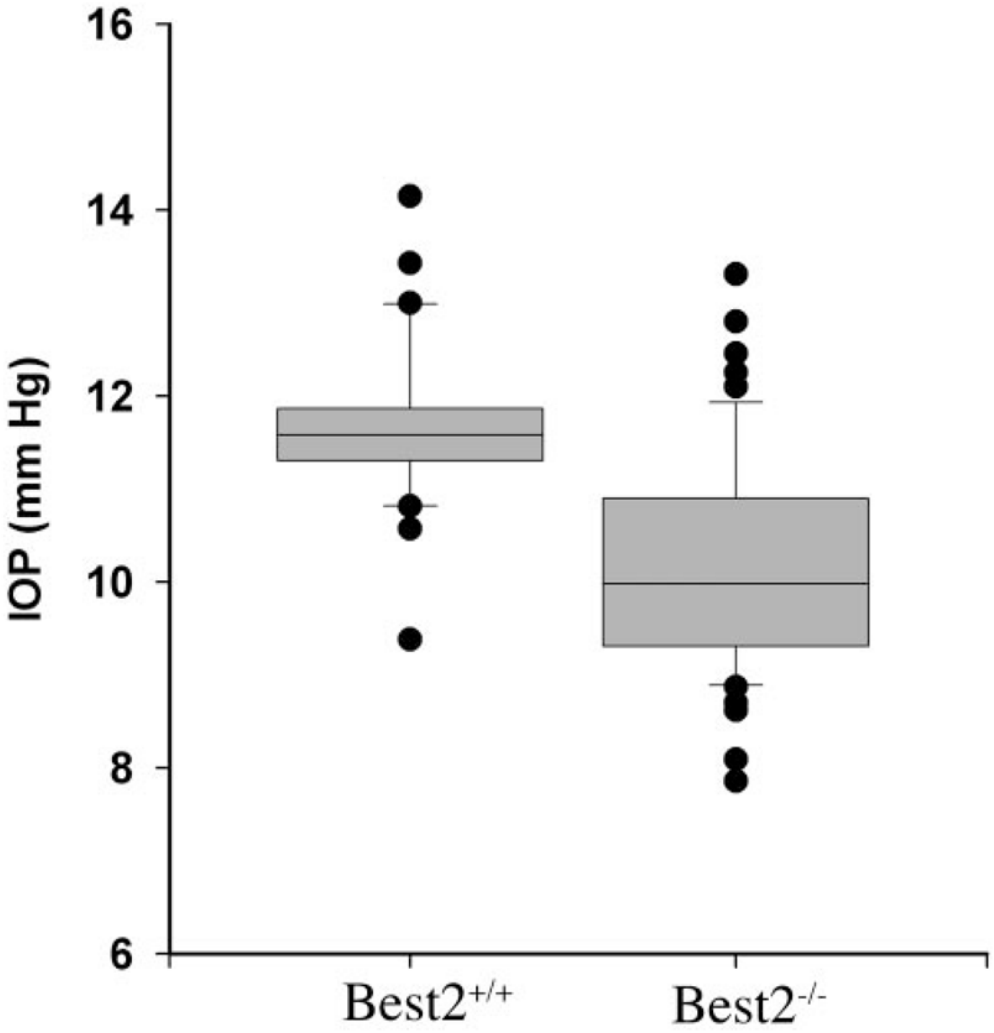

Figure 1.
Comparison of IOP in Best2$^{+/+}$ and *Best2*$^{-/-}$ mice. IOP was measured via anterior chamber cannulation. Note that IOP is significantly ($P < 0.0001$) lower in *Best2*$^{-/-}$ mice. Data are presented as a box plot in which the line within the box marks the median IOP, and the boundaries of the box indicate the range covered by the middle 50% of measurements. Bars above and below the boxes indicate the 90th and 10th percentiles, respectively. Symbols outside of the box and bars are outliers. *Best2*$^{+/+}$, $n = 31$; *Best2*$^{-/-}$, $n = 55$.

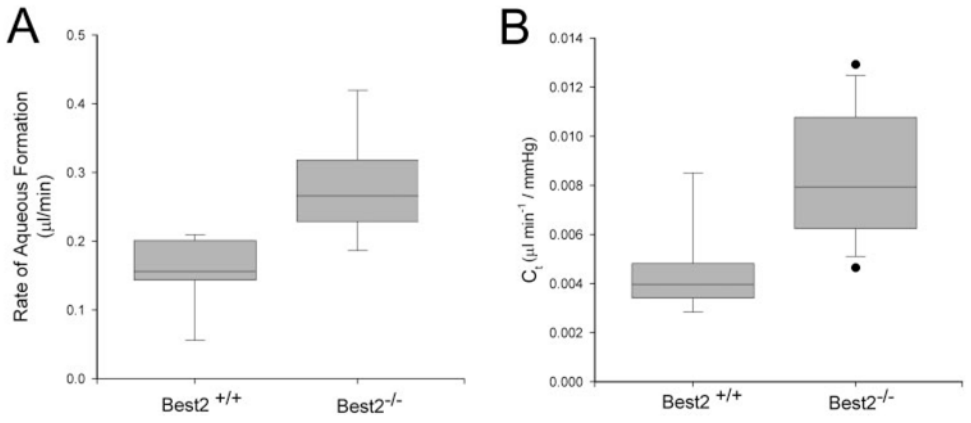

Figure 2.

Comparison of F_a (**A**) and C_t (**B**) in *Best2*$^{+/+}$ and *Best2*$^{-/-}$ mice. F_a is significantly ($P < 0.001$) elevated in *Best2*$^{-/-}$ mice compared with *Best2*$^{+/+}$ mice (**A**). C_t, is also elevated in *Best2*$^{-/-}$ mice compared with *Best2*$^{+/+}$ mice (**B**). Data are presented as a box plot in which the line within the box marks the median, and the boundaries of the box indicate the range covered by the middle 50% of measurements. Bars above and below the boxes indicate the 90th and 10th percentiles respectively. Symbols outside of the box and bars are outliers. *Best2*$^{+/+}$, $n = 9$ in (**A**) and 23 in (**B**); for *Best2*$^{-/-}$ $n = 9$ in (**A**) and 23 in (**B**).

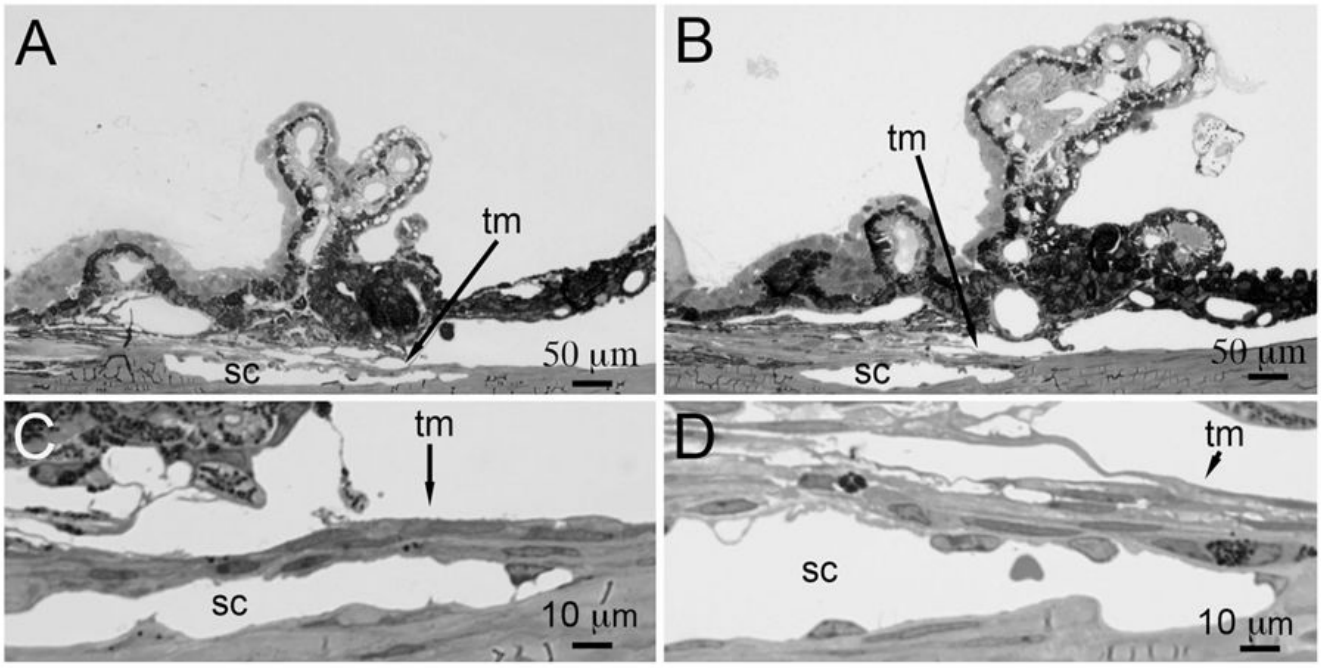

Figure 3.
Comparison of the angle in *Best2*$^{+/+}$ and *Best2*$^{-/-}$ mice. Representative photomicrographs of toluidine blue–stained thick sections of the angle in *Best2*$^{+/+}$ (**A**, **C**) and *Best2*$^{-/-}$ (**B**, **D**) mice. No significant differences were noted in the angle examined at low magnification (**A**, **B**). Inspection of Schlemm's canal (sc) and the trabecular meshwork (tm) at higher magnification (**C**, **D**) indicated little difference as well, although tm tissue was often more expanded in the *Best2*$^{-/-}$ mouse, perhaps indicative of a higher rate of flow through drainage tissues.

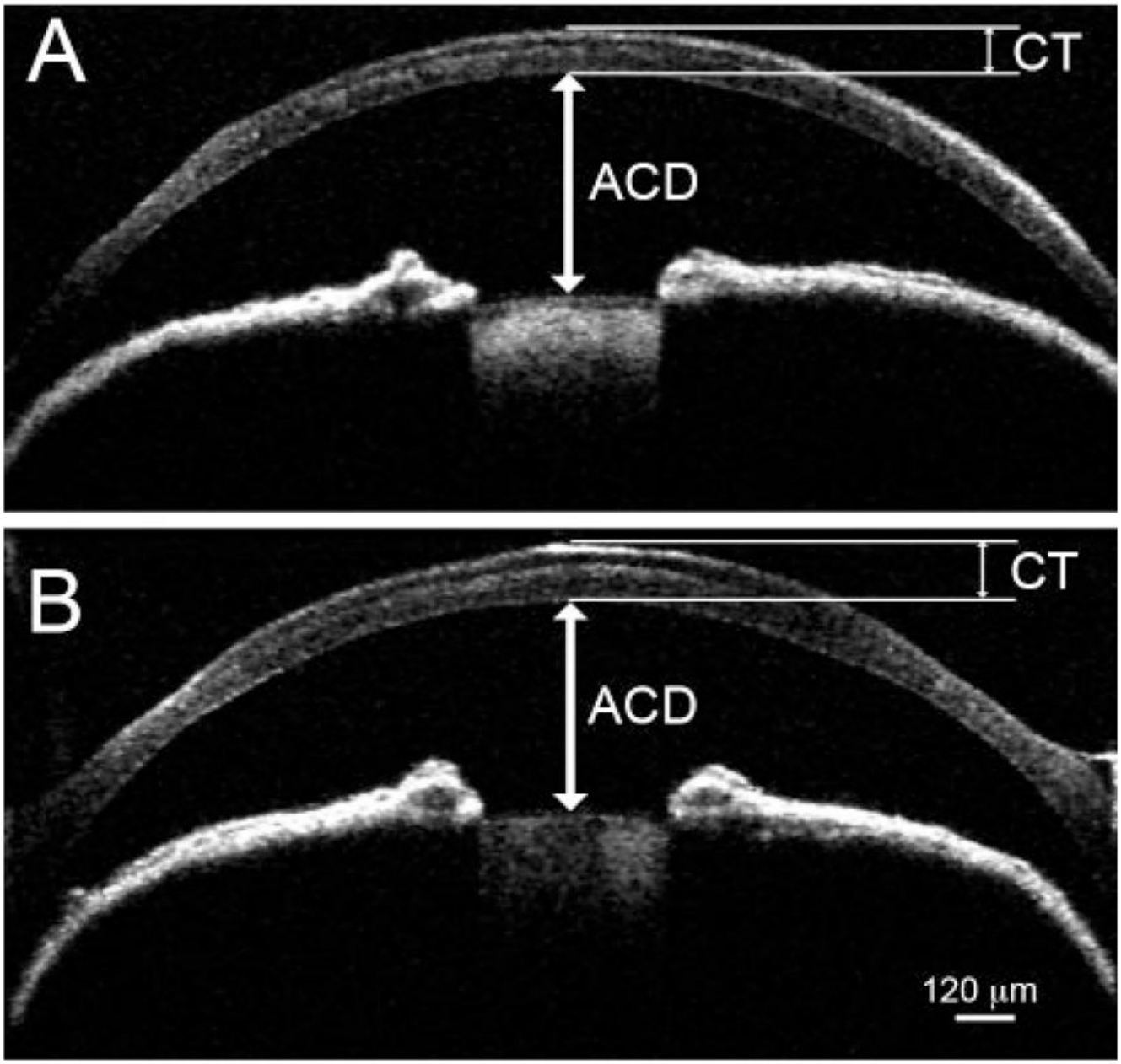

Figure 4.
OCT imaging of the anterior chamber of *Best2*$^{+/+}$ and *Best2*$^{-/-}$ mice. The anterior chambers of live *Best2*$^{+/+}$ (**A**) and *Best2*$^{-/-}$ (**B**) mice were examined using OCT. Anterior chamber depth (ACD) and corneal thickness (CT) were measured as indicated from images. On average, the ACD of *Best2*$^{-/-}$ mice was shallower than that of *Best2*$^{+/+}$ mice (see Table 2) with no significant difference in CT.

Table 1

Comparison of Aqueous Humor Dynamic Parameters of *Best2*$^{+/+}$ and *Best2*$^{-/-}$ Mice

	Best2$^{+/+}$			*Best2*$^{-/-}$		
Parameter*	**Data**	***n***	**Equation**	**Data**	***n***	**Equation**
IOP (mm Hg)	11.70 ± 0.16	31		10.22 ± 0.16	55	
EVP (mm Hg)	6.3 ± 0.3	9		6.3 ± 0.3	9	
F_a (μL/min)	0.160 ± 0.047	9	1	0.277 ± 0.069	9	1
C_t (μL · min^{-1}/mm Hg)	0.0050 ± 0.0015	23	2	0.0085 ± 0.0026	23	2
F_c (μL/min)	0.027		3	0.033		3
F_u (μL/min)	0.133		4	0.244		4
V_a (μL)	4.51 ± 0.37	8		3.74 ± 0.27	12	
Turnover rate (%· min^{-1})	3.5		5	7.4		5

Data are presented as the mean ± SD, except for IOP where data are the mean ± SE.

*Values for F_C, F_U, and turnover rate were derived form measured data using the indicated equations.

Table 2

Structural Attributes of the Anterior Chamber of *Best2*$^{+/+}$ and *Best2*$^{-/-}$ Mice

	Anterior Chamber Depth (μm)*	Corneal Thickness (μm)
Best2$^{+/+}$ (*n* =12)	496 ± 27	100 ± 16
Best2$^{-/-}$ (*n* =15)	458 ± 17	101 ± 13

Data are expressed as the mean ± SD.

*$P < 0.001$.